


A Comparison of Automated Perfusion- and Manual Diffusion-Based Human Regulatory T Cell Expansion and Functionality Using a Soluble Activator Complex

Cell Transplantation
Volume 29: 1–15
© The Author(s) 2020
Article reuse guidelines:
sagepub.com/journals-permissions
DOI: 10.1177/0963689720923578
journals.sagepub.com/home/ctj


Mark Jones¹ , Brian Nankervis¹, Kelly Santos Roballo²,
Huong Pham², Jared Bushman², and Claire Coeshott¹

Abstract

Absence or reduced frequency of human regulatory T cells (Tregs) can limit the control of inflammatory responses, autoimmunity, and the success of transplant engraftment. Clinical studies indicate that use of Tregs as immunotherapeutics would require billions of cells per dose. The Quantum[®] Cell Expansion System (Quantum system) is a hollow-fiber bioreactor that has previously been used to grow billions of functional T cells in a short timeframe, 8–9 d. Here we evaluated expansion of selected Tregs in the Quantum system using a soluble activator to compare the effects of automated perfusion with manual diffusion-based culture in flasks. Treg CD4⁺CD25⁺ cells from three healthy donors, isolated via column-free immunomagnetic negative/positive selection, were grown under static conditions and subsequently seeded into Quantum system bioreactors and into T225 control flasks in an identical culture volume of PRIME-XV XFSM medium with interleukin-2, for a 9-d expansion using a soluble anti-CD3/CD28/CD2 monoclonal antibody activator complex. Treg harvests from three parallel expansions produced a mean of 3.95×10^8 (range 1.92×10^8 to 5.58×10^8) Tregs in flasks (mean viability 71.3%) versus 7.00×10^9 (range 3.57×10^9 to 13.00×10^9) Tregs in the Quantum system (mean viability 91.8%), demonstrating a mean 17.7-fold increase in Treg yield for the Quantum system over that obtained in flasks. The two culture processes gave rise to cells with a memory Treg CD4⁺CD25⁺FoxP3⁺CD45RO⁺ phenotype of 93.7% for flasks versus 97.7% for the Quantum system. Tregs from the Quantum system demonstrated an 8-fold greater interleukin-10 stimulation index than cells from flask culture following restimulation. Quantum system-expanded Tregs proliferated, maintained their antigenic phenotype, and suppressed effector immune cells after cryopreservation. We conclude that an automated perfusion bioreactor can support the scale-up expansion of functional Tregs more efficiently than diffusion-based flask culture.

Keywords

regulatory T cells, Tregs, cell expansion, Quantum, automation, immunotherapy

Introduction

Human regulatory T cells (Tregs) play a central role in the maintenance of self-tolerance, transplantation tolerance, and suppression of autoimmune responses but are found at a frequency of only 4%–6% of cluster of differentiation 4 (CD4⁺) T cells or 1%–2% of lymphocytes in peripheral blood^{1,2}. The absence or reduced frequency of Tregs can limit the control of immune inflammatory responses, autoimmunity, and the success of transplant engraftment^{3,4}. Clinical studies indicate that the use of Tregs as immunotherapeutics would require billions of cells per dose;

¹ Terumo BCT, Inc, Lakewood, CO, USA

² School of Pharmacy, University of Wyoming, Laramie, WY, USA

Submitted: November 12, 2019. Revised: March 26, 2020. Accepted: April 7, 2020.

Corresponding Author:

Mark Jones, Terumo BCT, Inc, 10810 West Collins Avenue, Lakewood, CO 80215, USA.

Email: mark.jones@terumobct.com



Creative Commons Non Commercial CC BY-NC: This article is distributed under the terms of the Creative Commons Attribution-NonCommercial 4.0 License (<https://creativecommons.org/licenses/by-nc/4.0/>) which permits non-commercial use, reproduction and distribution of the work without further permission provided the original work is attributed as specified on the SAGE and Open Access pages (<https://us.sagepub.com/en-us/nam/open-access-at-sage>).

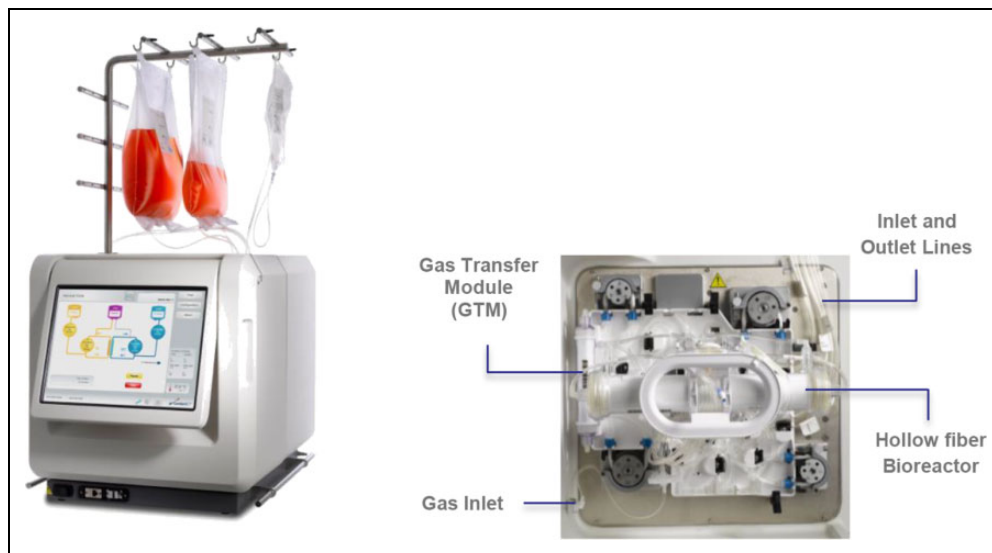


Figure 1. Automated Quantum Cell Expansion System (left) showing the graphic user interface (left) and internal view (right) showing the disposable set containing the hollow fiber bioreactor and the gas transfer module. This figure is a derivative of an image of the Quantum system (© Terumo BCT, Inc., 2013).

for example, recent phase I studies by Mathew et al. used Treg doses in the range of 0.5×10^9 to 5.0×10^9 cells to facilitate kidney transplantation, and clinical studies by Bluestone et al. indicated that polyclonal Treg doses in the range of 5×10^6 to 2.6×10^9 cells were well tolerated in type 1 diabetes patients^{5,6}.

The Quantum[®] Cell Expansion System (Quantum system, Cat. 92000, Terumo BCT, Inc., Lakewood, CO, USA) is a functionally closed, automated, hollow-fiber bioreactor system that has previously been used to grow billions of functional T cells in 8–9 d⁷ and represents a potential solution for the expansion of human T cells, which may be utilized in the treatment of numerous types of cancer and other disorders. The Quantum system (Fig. 1) consists of a synthetic hollow-fiber bioreactor that is part of a sterile closed-loop circuit for media and gas exchange. The bioreactor and fluid circuit comprise a single-use disposable set that is mounted on the Quantum system. The bioreactor itself contains 11,520 hollow fibers with a total intracapillary (IC) surface area of 2.1 m² and 124 ml of fluid volume within the fibers of the bioreactor. The IC compartment is separated from the extracapillary (EC) compartment by a semipermeable polyethersulfone membrane. Gas control is also managed using hollow-fiber technology in a gas transfer module with a surface area of 0.16 m². In Quantum system culture, perfusion feeding, improved gas exchange, and efficient removal of lactate were previously shown to increase the yield of human peripheral blood mononuclear cell-derived T cells from an average of 10.8×10^9 to more than 28×10^9 in only 10 d^{7,8}. In order to further evaluate the capability of the Quantum system, the current comparative study was designed to evaluate the growth of Tregs in the Quantum

system two-compartment bioreactor versus the static conditions in tissue culture polystyrene T225 flasks.

Enrichment of human Tregs prior to expansion is central to the overall process since it is important not only to increase the number of CD4⁺CD25⁺CD127⁻FoxP3⁺ T cells but also to reduce the number of CD127⁺ effector T cells. For Tregs, the forkhead box protein P3 (FoxP3) is the key transcriptional factor that activates cytotoxic T lymphocyte-associated protein 4 (CTLA-4) and the interleukin-2 receptor (IL-2R) and represses IL-2 and interferon- γ to promote immunological homeostasis. Moreover, FoxP3 expression inversely correlates with CD127 in human Tregs⁹. Previously, immunomagnetic column enrichment processes for Tregs have resulted in only 40%–60% Treg recovery from peripheral blood, and these collections can be contaminated with CD127⁺ effector T cells^{10,11}. Therefore, we have taken the approach to expand peripheral blood-derived Tregs isolated by an immunomagnetic column-free negative/positive selection method that depletes undesirable cells and enriches for a Treg population with higher FoxP3 expression¹². This method also allowed us to expand Tregs without the use of rapamycin (an inhibitor of the mammalian target of rapamycin—mTOR—a regulator of translation and cell size), which is typically used to suppress proinflammatory T cell contamination and to preserve levels of FoxP3 expression^{13–21}.

We also chose to focus our protocol development on the ex vivo expansion of selected Tregs in the Quantum system using a soluble activator, an anti-CD3/CD28/CD2 monoclonal antibody (mAb) activator complex. CD4⁺CD25⁺ Treg cells, enriched by negative/positive selection by the vendor, from three unrelated healthy donors, were grown under static conditions and subsequently seeded into Quantum system

bioreactors and into T225 control flasks for scale-up expansion over 9 d to compare the effects of automated perfusion with manual diffusion-based culture. Cell growth, viability, phenotype, and cytokine secretion profiles of the expanded Tregs were compared. In addition, the suppressive capacity of Quantum system-expanded Tregs was measured in a rat splenocyte proliferation assay.

Materials and Methods

In order to support the overall goals of cell therapy development, the guidelines in the publication “Minimum information about T regulatory cells (MITREG): A step toward reproducibility and standardization” were consulted for this study²² and followed where applicable.

Donor Cells and Treg Enrichment

Human peripheral blood CD4⁺CD25⁺ Tregs were purchased from STEMCELL Technologies (Vancouver, BC, Canada). The vendor had previously isolated Tregs from peripheral blood mononuclear cells (PBMCs) of healthy donors using column-free EasySep (Cat. 18063, STEMCELL Technologies) negative/positive immunomagnetic separation techniques which involved the removal of CD8⁺ T cells and the selection of CD25⁺ cells from PBMCs. Donor cells were collected by the vendor, STEMCELL Technologies, in accordance with local, state, and federal U.S. requirements, from normal or noninfectious diseased donors voluntarily participating in a donor program with consent that was approved by an institutional review board, Food and Drug Administration (FDA), or an equivalent regulatory agency, and were negative for human immunodeficiency virus-1 and -2 and hepatitis B and C viruses. Purity by flow cytometry was $\geq 85\%$ CD4⁺CD25⁺ Tregs and viability was $>80\%$.

Automated Treg Expansion

Complete medium for the IC loop of the Quantum system was composed of PRIME-XV T-Cell Expansion XFSM medium, a xenogeneic component-free (without the use of nonhuman components), serum-free medium (PRIME-XV, Fujifilm Irvine Scientific, Santa Ana, CA, USA), penicillin-streptomycin-neomycin antibiotic mixture (Thermo Fisher Scientific, Carlsbad, CA, USA), and 100 IU/ml of recombinant human IL-2 improved sequence (Miltenyi Biotec, Auburn, CA, USA). For the initial Treg inoculum cell preparation in the automated Treg expansion arm, donor cells were first seeded at 1×10^5 to 3×10^5 cells/ml in flasks in complete medium, stimulated (see below), and grown for 9 d to permit cell recovery from cryopreservation. On day 9 of the inoculum preparation (day 0 of the comparative expansion study), the Quantum system IC side of the disposable set (Terumo BCT, Lakewood, CO, USA) was seeded with 3.0×10^7 Tregs in 124 ml of complete medium, and Immunocult

Human CD3/CD28/CD2 T Cell Activator (STEMCELL Technologies, Vancouver, BC, Canada) was added to the complete medium at 25 μ l/ml medium (based on the IC loop volume, which includes the bioreactor volume of 124 ml), to stimulate the growth of Tregs. Base medium was composed of PRIME-XV medium and antibiotics and was used to manage metabolite concentrations and gas exchange in the EC loop of the two-chambered Quantum system bioreactor. Both complete (IC) medium and base (EC) medium were stored at 4°C–6°C prior to use and the IC medium was also protected from light during use. Tregs in the flask and the Quantum system were incubated at 37°C with a gas mixture of 5% CO₂ and 5% CO₂/20% O₂/balance N₂, respectively. Complete medium was initially added to the bioreactor cultures via continuous perfusion at 0.1 ml/min to the IC loop⁷. Perfusion rates to the IC loop containing the bioreactor were increased incrementally up to 0.4 ml/min in order to maintain lactate concentrations below 10 mmol/l. EC medium perfusion rates in the Quantum system were adjusted independently up to 2.0 ml/min to further control lactate levels. Beginning on day 3, Tregs were circulated through the IC loop at 300 ml/min for 4 min during the bolus base medium feeding task to disassociate cell aggregates and return the cell suspension to the hollow fibers of the bioreactor through bidirectional reseeded for base/complete media perfusion additions. Cells were harvested automatically on day 9 under aseptic conditions by circulating the cells through the IC loop of the rotating (–90° to 180°) bioreactor at a flow rate of 300 ml/min for 4 min to disassociate aggregated cells or microcolonies. This step in the harvest task was followed by collection in the system harvest bag at IC/EC flow rates of 100 ml/min for 4 min with medium without supplements as previously described. During cell harvest, the preprogrammed IC media flow was divided at a ratio of 80:20 to capture cells from both segments of the IC loop of the bioreactor prior to entering the preattached harvest bag. At this point, the harvest bag tubing was radio frequency-sealed and the expanded cell harvest was removed aseptically from the system for subsequent analysis, downstream processing, or cryopreservation. Cell harvest numbers and viability were measured by Vi-CELL XR automated cell counter (Beckman Coulter, Indianapolis, IN, USA) using trypan blue exclusion (Cat. 383260, Beckman Coulter Vi-CELL Reagent Pak). Cells were subsequently cryopreserved at 2.0×10^7 cells/ml in CryoStor CS10 (BioLife Solutions Inc., Bothell, WA, USA), stored overnight at 80°C in CoolCell freezing containers (Corning Inc., Corning, NY, USA), and subsequently transferred to liquid nitrogen vapor phase for long-term cryopreservation until further analysis.

Manual Treg Expansion

For the Treg inoculum cell preparation in the manual Treg expansion arm, donor cells were seeded in flasks at 1×10^5 to 3×10^5 cells/ml in complete medium, stimulated (see below), and grown for 9 d to permit cell recovery from

cryopreservation. On day 9 of the inoculum preparation (day 0 of the comparative expansion study), vented T225 tissue culture flasks (Corning Inc.) for the manual arm were seeded with 3.0×10^7 Tregs in 124 ml of complete medium and Immunocult Human CD3/CD28/CD2 T Cell Activator was added at 25 μ l/ml medium (based on a flask volume of 124 ml). Flasks were incubated at 37°C in a humidified incubator at 5% CO₂ under static conditions. Complete medium was changed every 2 d after seeding (day 0). Beginning on day 3, flask-expanded cell cultures were centrifuged at $500 \times g$ for 5 min, spent medium was aspirated, and cells were resuspended in 124 ml complete medium. Cells were manually disassociated and removed from flasks by serological pipet and subsequently centrifuged as before prior to counting and cryopreservation as described above.

Calculation of Population Cell Doublings and Cell Doubling Time

For the purposes of this study, population cell doublings (DS) and cell doubling time (DT) were estimated in terms of the standard exponential growth equation over the period of cell expansion as derived from Sherley²³.

Population Cell Doubling (DS) where LN is the natural logarithm :

$$DS = [\text{LN}(\text{harvested cells} \div \text{seeded cells})] \div \text{LN}(2)$$

Population Cell Doubling Time (DT in hours (h))

where LN is the natural logarithm :

$$DT = [\text{LN}(2) \times \text{day} \times 24] \div \text{LN}(\text{harvested cells} \div \text{seeded cells})$$

Treg Metabolism

Lactate and glucose measurements were taken daily (day 0 through day 9) with i-STAT handheld blood analyzers (Abbott Point of Care, Princeton, NJ, USA) using CG4+ and G cartridges, respectively. Samples were obtained from the EC sample port during Quantum system cell expansions.

Treg Phenotyping

Flow cytometry was performed at the Human Immune Monitoring Shared Resource, University of Colorado School of Medicine, Aurora, CO, USA. Thawed Tregs from flask and Quantum system harvests were stained with respective fluorochrome conjugates as previously described⁷ using Zombie Green Fixable Viability stain (BioLegend, San Diego, CA, USA) and the following directly conjugated mAbs: Brilliant Violet 786 mouse antihuman CD3 mAb, Brilliant Ultraviolet 395 mouse antihuman CD4 mAb, Brilliant Ultraviolet 737 mouse antihuman CD8 mAb, Allophycocyanin-eFluor 780 mouse antihuman CD45RO mAb (all from BD Biosciences, San Jose, CA, USA), Phycoerythrin antihuman CD25 mAb, and Alexa Fluor 647 mouse antihuman FOXP3 mAb (both

from BioLegend). Data were collected on a BD FACS LSRFortessa X-20 flow cytometer (Cat. 657669) and analyzed by BD FlowJo Software (v10.5.3). Each flow sample contained 50,000 events and was processed using fluorescence minus one (FMO) gating. Treg frequency was based on the number of CD4⁺CD25⁺FOXP3⁺ cells within the CD25⁺FOXP3⁺ double-positive gate that were above background FMO fluorescence.

Treg Cytokine Secretion

Cytokine secretion assays were performed at the Human Immune Monitoring Shared Resource, University of Colorado School of Medicine. Cryopreserved Tregs from Quantum system and flask expansions were thawed at 37°C and were either left unstimulated or were restimulated with soluble activator (Immunocult Human CD3/CD28/CD2 T Cell Activator) in complete medium and incubated (37°C, 5% CO₂, humidity) for 4 d to compare automated perfusion culture with manual diffusion-based culture for inhibitory cytokine secretion by Tregs. Cell culture supernatants were analyzed in triplicate for the presence of IL-10 and transforming growth factor (TGF)- β 1 by sulfo-tag electrochemiluminescence (Meso Scale Diagnostics, Rockville, MD, USA) using mouse antihuman IL-10 mAb and mouse antihuman TGF- β 1 mAb conjugates, respectively. Background values were subtracted from raw data and a stimulation index was calculated for the expanded Tregs by dividing the cytokine concentration derived from the stimulated sample (pg/ml) by the concentration from the unstimulated sample (pg/ml).

Xenogeneic In Vitro Suppression by Tregs

The functionality of Tregs harvested from the Quantum systems was evaluated by the ability to suppress proliferation in a xenogeneic splenocyte assay. Tregs used for the rat splenocyte suppression assay were independently phenotyped at the University of Wyoming (Laramie, WY, USA) as previously described²⁴. In order to prepare the Tregs for the suppression assay, post-thaw viability and growth were measured. Cryopreserved Tregs were thawed by placing vials in a 37°C water bath for 5–10 min until no ice was left in the vial. The contents of the vial were transferred to a 15-ml conical tube with Treg medium consisting of RPMI 1640 (Sigma-Aldrich Corp., St. Louis, MO, USA) containing 10% fetal bovine serum (FBS, Thermo Fisher Scientific, Gibco), 100 U/ml penicillin (Thermo Fisher Scientific), 100 μ g/ml streptomycin (Thermo Fisher Scientific), 50 μ M β -mercaptoethanol (Sigma-Aldrich Corp.), and 400 IU/ml IL-2 (R&D Systems, Minneapolis, MN, USA). Tubes were centrifuged at $300 \times g$ for 5 min, supernatant was discarded, and pellets were resuspended with fresh Treg medium.

To measure the growth curve, Tregs were seeded at a density of 2×10^6 cells per well in a 6-well plate (Greiner Bio-One N.A., Monroe, NC, USA) coated with goat

antimouse IgG antibody (Thermo Fisher Scientific) and mouse anti-CD28 mAb (BD Biosciences) at respective concentrations of 5 and 10 $\mu\text{g/ml}$, as previously described²⁴. The number of viable cells was counted by trypan blue exclusion at each time point using a Neubauer chamber (Cat. 5971R30, Hausser Scientific, Horsham, PA, USA) and visualized with 10 \times light microscopy (Evos XL core microscope, Invitrogen-ThermoFisher Scientific, Grand Island, NY, USA). Cells grown for 5 and 13 d were subsequently used in the suppression assay (see below).

Animals. Sprague Dawley rats constitutively expressing green fluorescent protein (GFP) were acquired from the Rat Resource and Research Center (Columbia, MO, USA; strain SD-Tg(UBC-EGFP) 2BalRrrc). SD-Tg(UBC-EGFP) 2BalRccc are transgenic rats that express enhanced green fluorescent protein (EGFP) from the ubiquitin C promoter in all cells^{25,26}. Animals were acquired, cared for, and used in accordance with the NIH Guide for the Care and Use of Laboratory Animals and followed a protocol approved by the University of Wyoming Institutional Animal Care and Use Committee. Rats were housed at ambient temperature with stable humidity and natural day–night cycle, with free access to rodent laboratory food and water.

Proliferation Assay. Assays were carried out as previously described²⁴. Briefly, Tregs were thawed and expanded as described above and then cocultured with isolated splenocytes from GFP rats. Three days prior to coculture, GFP rat splenocytes were stimulated with 5 $\mu\text{g/ml}$ concanavalin A (con A; Sigma-Aldrich Corp.). Tregs were mixed with 20,000 con A–stimulated GFP rat splenocytes at ratios of 1:1, 1:2, 1:4, 1:6, 1:8, and 1:16 splenocytes to Tregs (day 0 of co-culture) and proliferation of splenocytes was measured over a 4-d period by GFP fluorescence using a Tecan M200 plate reader (Tecan Group Ltd, Männedorf, Switzerland). Co-culture was carried out in RPMI 1640, 10% FBS, 100 U/ml penicillin, 100 $\mu\text{g/ml}$ streptomycin, and 50 μM β -mercaptoethanol in 96-well plates. Measurement of proliferation from con A–stimulated GFP splenocytes alone was used as the control. The *in vitro* suppression assay was performed using Tregs from each donor separately after 5 or 13 d of monoculture following thawing. Correlation of rat splenocyte fluorescence in co-culture with Quantum system–expanded Tregs was calculated and averaged across all three donor cell products by subtracting the fluorescence units from splenocytes with no Tregs from the maximum suppression at day 4 (1:1 ratio of splenocytes to Tregs).

Phenotype of Cryopreserved Tregs by Microscopy. Thawed Tregs were cultured for 13 d prior to measuring the immunophenotype. After passaging, 10 \times 10⁶ Tregs from each donor were washed with phosphate-buffered saline (Sigma-Aldrich Corp.) and labeled with PE-antihuman CD4 mAb (1:50; Thermo Fisher Scientific) and Alexa 488-antihuman CD25 mAb (1:50; Thermo Fisher Scientific), then

permeabilized with 0.1% Triton X-100 (Cat. T8787-100ML, Sigma-Aldrich, St. Louis, MO, USA), and labeled with PE antihuman FoxP3 mAb (1:100; BD Biosciences) and 4',6-diamidino-2-phenylindole (Cat. MBD0015-1ML, Sigma-Aldrich, 0.01 mg/ml). Labeling was performed in triplicate for Tregs from each donor. Labeled cells were mounted on coverslips with Fluoroshield (Sigma-Aldrich Corp.) and imaged by fluorescence microscopy (EVOS FL, Life Technologies, and Zeiss 710 confocal microscope, Carl Zeiss Microscopy LLC, White Plains, NY, USA). The total cell number and positive cells for each marker were manually counted. The percentage of positive cells per marker was calculated from the number of positive cells (\times 100) divided by the total cell number. An average of 15 fields was randomly imaged for each cell population that was labeled, where the total number of cells quantified within each set of 15 fields averaged 14,400. Cell counts were performed manually by individuals blinded to the experimental donors.

Statistical Analysis

Descriptive statistics included the calculation of mean, range, and standard error of the mean (s.e.m.). *P* values were calculated using Student's *t*-test over a confidence interval of 95%, unless otherwise stated. Correlation coefficients were calculated by *R*² analysis.

Results

Treg Expansion

Actively growing, enriched CD4⁺CD25⁺ human Tregs from three healthy donors were expanded over 9 d (8.6–8.8 d) in parallel flask diffusion–based and Quantum system perfusion–based culture. Over the course of the expansion study, Treg yields were consistently higher in the Quantum system arm versus those in the flask arm. The mean harvest yields were 3.95 \times 10⁸ cells (range 1.92 \times 10⁸ to 5.58 \times 10⁸) for the manual flask expansion and were 7.00 \times 10⁹ cells (3.57 \times 10⁹ to 1.30 \times 10¹⁰) for the automated Quantum system expansion (Fig. 2A). The corresponding population doublings were 3.6 (range 2.7–4.2) for the flask expansion versus 7.6 (range 6.9–8.8) for the Quantum system. The mean population doubling time for the flask-based cell culture was 60.5 h (range 48.9–78.0 h) versus 27.8 h (range 23.6–30.3 h) for the Quantum system–based cell culture. At harvest, the cell density averaged 3.19 \times 10⁶ cells/ml (range 1.55 \times 10⁶ to 4.50 \times 10⁶ cells/ml) for the flask expansions and 56.4 \times 10⁶ cells/ml (range 28.8 \times 10⁶ to 105.0 \times 10⁶ cells/ml) for the Quantum system expansions. Overall, the enriched Tregs from the three donor populations expanded 10-fold to 23-fold more under perfusion culture than those expanded under diffusion culture. Harvest cell viability averaged 71.3% (range 56.8%–80.5%) in the flask expansion arm and 91.8% (range 89.4%–93.7%) in the Quantum system expansion arm. These data suggest that there is a trend toward

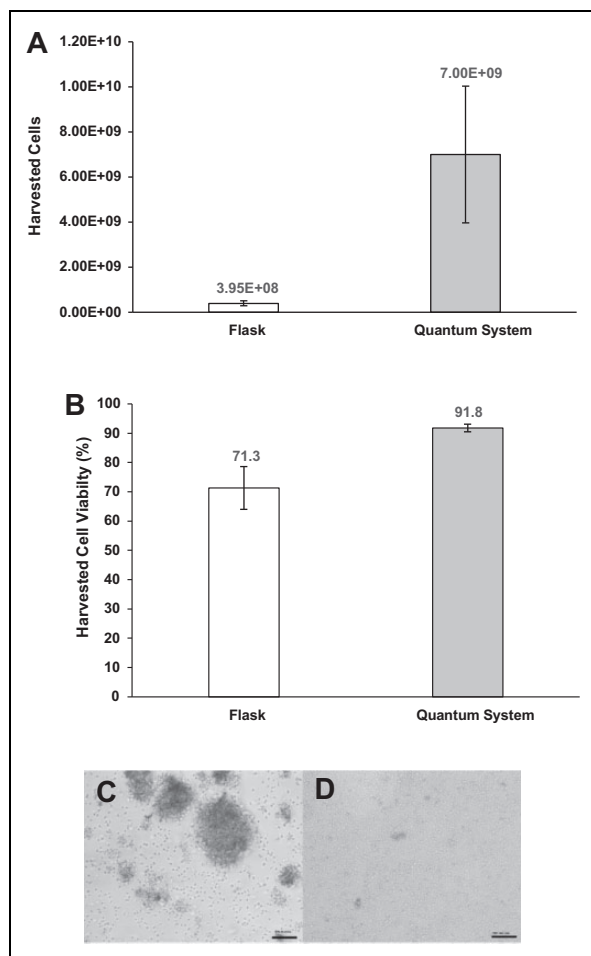


Figure 2. Total Treg harvest for flask diffusion-based and Quantum system perfusion-based cell culture protocols. Total Treg harvest, $P = 0.10$ (A). Harvested cell viability for flask diffusion-based and Quantum system perfusion-based cell culture protocols, $P = 0.05$ (B). Representative Treg morphology from flask harvest (C). Representative Treg morphology from Quantum system harvest (D). Reference bar 100 μm . Magnification: 100 \times . Tregs: regulatory T cells.

higher Treg harvest viability in the perfusion-based culture versus diffusion-based culture, as the difference in the means was found to be informative, but not statistically significant ($P = 0.05$, Fig. 2B).

Although cell aggregation can be indicative of Treg stimulation, it can also potentially limit nutrient transport and waste product exchange to cells in the center of an aggregate during expansion²⁷. For this reason and to limit aggregation, Tregs cultured in the Quantum system were circulated daily through the IC loop beginning on day 3. In the flask arm, the cells were processed by pipet every 2 d during media exchange beginning on day 3 and continuing until just before cell harvest on day 9. The Treg morphology images after harvest reflect the presence of aggregated cells in the flask arm, whereas there was little evidence of aggregation in the Quantum system arm (Fig. 2C, D).

Treg Metabolism

Over the course of the 9-d expansion of Tregs in the Quantum system, glucose consumption rates reached a maximum of 24.3 mmol/d in the cells from all three donors over the automated composite IC/EC media flow rates of 0.1–2.4 ml/min (Fig. 3A, B). Glucose concentration ranged from 383 to 279 mg/dl in donor 1 Tregs, from 381 to 347 mg/dl in donor 2 Tregs, and from 379 to 341 mg/dl in donor 3 Tregs from day 0 to day 9. During the culture process, the range of glucose consumption rates reflected both the exponential growth and the donor variability associated with activated Treg expansion. At harvest, the glucose consumption rate in mmol/d in the Quantum system correlated ($R^2 = 0.9967$) with the cell yield across the three donor Treg populations (Fig. 3G).

Over the same time course, lactate generation rates from Tregs grown in the Quantum systems reached a maximum of 37.23 mmol/d for the three donor products over the IC/EC media flow rates of 0.1–2.4 ml/min (Fig. 3C, D). During the culture process, lactate concentration ranged from 0 to 9.04 mmol/l in donor 1 Tregs, from 0 to 3.90 mmol/l in donor 2 Tregs, and from 0 to 3.87 mmol/l in donor 3 Tregs. Similar to glucose consumption, the range of lactate generation rates also reflected both the exponential growth and the donor variability associated with activated Treg expansion. At harvest, the lactate generation rate in mmol/d in the Quantum system correlated ($R^2 = 0.9942$) with the cell yield across the three donor Treg populations (Fig. 3H).

To adjust the automated perfusion system, the 1:2 ratio of glucose to lactate molecules can be used to define an upper limit for lactate generation in mmol/d via EC medium sampling, at which point media flow rates (ml/min) can be adjusted based on the level of glycolysis during cell expansion. In this study of Treg expansion, the combined Quantum system IC and EC medium flow rates ranged from 0.1 to 2.4 ml/min while keeping the ratio of lactate to glucose on average $\leq 1:1.8$ over the three donor expansions (Fig. 3E, F).

Treg Phenotype

Cells harvested from flasks and Quantum systems were evaluated for Treg phenotype by flow cytometry (Table 1A). The Treg flow cytometry gating strategy is outlined in Fig. 4. The Treg phenotype $\text{CD4}^+\text{CD25}^+\text{FoxP3}^+$ averaged 76.5% (range 69.9%–84.1%) of the total population for cells grown in flasks and 80.3% (range 77.0%–82.2%) for cells grown in the Quantum system (Table 1A). In addition to confirming the fundamental Treg phenotype, the frequency of memory Treg was also analyzed for all products (Table 1B). The results demonstrated that the majority of the expanded Tregs displayed a memory phenotype of $\text{CD3}^+\text{CD4}^+\text{FoxP3}^+\text{CD45RO}^+$ with a mean population frequency of 93.7% (range 90.3%–95.4%) for Tregs grown in flasks and 97.7% (range 97.1%–98.3%) for Tregs in the Quantum system. Although the difference between the flask and Quantum system memory Tregs frequency was not

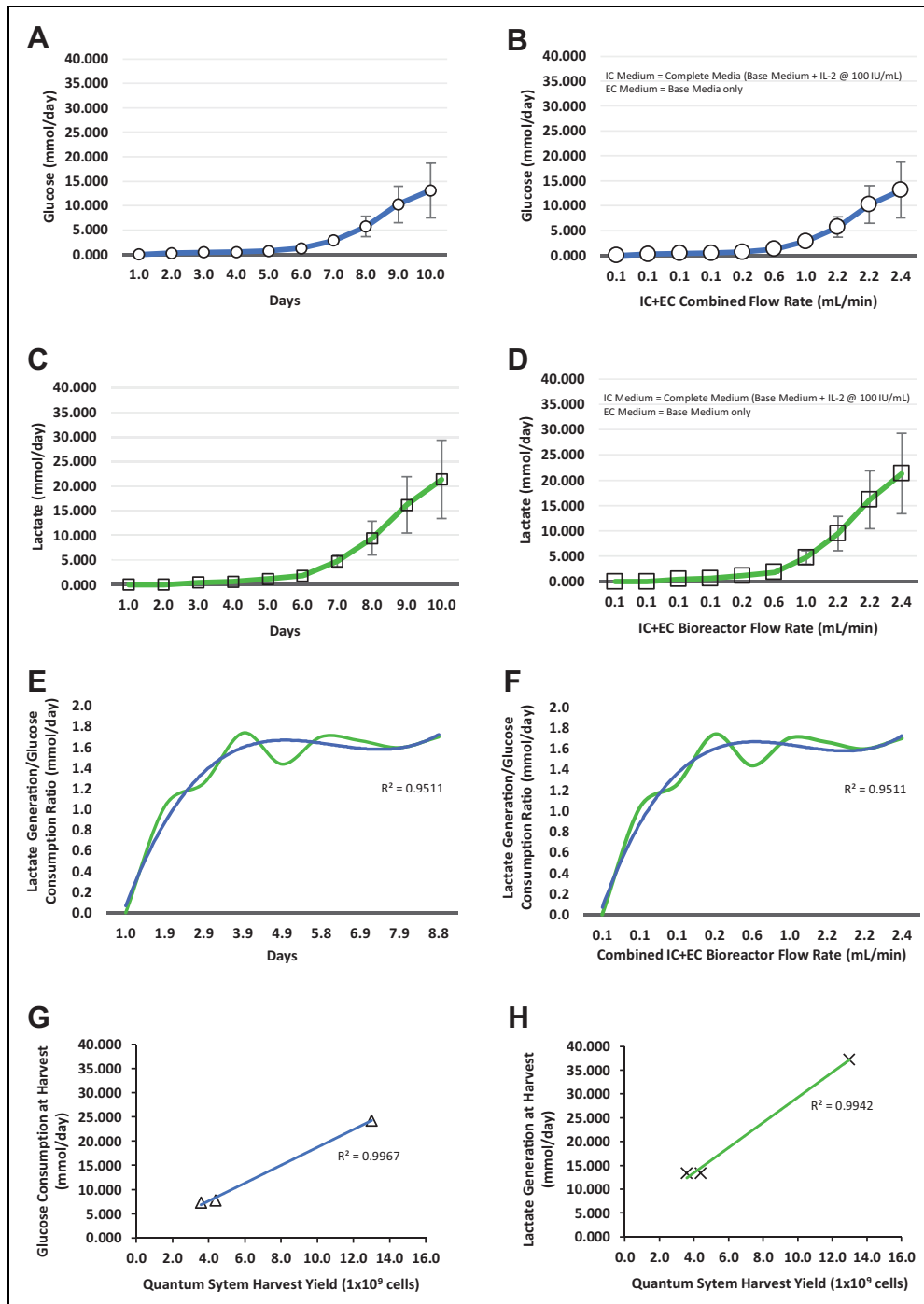


Figure 3. Treg metabolites for the Quantum system expansion. Glucose consumption with respect to culture time (A) and total media flow rates (B), lactate generation with respect to culture time (C) and total media flow rates (D), lactate/glucose ratio with respect to culture time (E), and total media flow rates (F), correlation of Quantum system harvest yield with glucose consumption (G), and correlation of Quantum system harvest yield with lactate generation (H). (A–D) Cell expansions from individual donors; (E, F) means of cell expansions from three donors (blue = trendline; green = mean of lactate/glucose mmol/d). EC: extracapillary; IC: intracapillary; Tregs: regulatory T cells.

statistically significant, there was a trend toward a higher frequency of a memory phenotype in perfusion cell culture (Table 1B).

Treg Cytokine Secretion

Cryopreserved cells from both flask and Quantum system expansions were thawed, washed, resuspended in complete

Table 1A. Treg Phenotype at Harvest in Diffusion-Based Flask and Perfusion-Based Quantum System Cell Culture.

Treg source	Flask CD4 ⁺ CD25 ⁺ FoxP3 ⁺ Treg frequency (%)	Quantum system CD4 ⁺ CD25 ⁺ FoxP3 ⁺ Treg frequency (%)
Donor 1	84.1	81.7
Donor 2	75.6	77.0
Donor 3	69.9	82.2
Mean	76.5	80.3
s.e.m.	4.1	1.7

Mean Treg frequency with s.e.m. CD4, CD25: clusters of differentiation 4 and 25; FoxP3: forkhead box protein P3; s.e.m.: standard error of the mean; Tregs: regulatory T cells.

Table 1B. Memory Treg Phenotype at Harvest in Flask Diffusion-Based and Quantum System Culture.

Treg source	Flask Memory Tregs CD3 ⁺ CD4 ⁺ FoxP3 ⁺ CD45RO ⁺ (%)	Quantum system Memory Tregs CD3 ⁺ CD4 ⁺ FoxP3 ⁺ CD45RO ⁺ (%)
Donor 1	95.3	98.3
Donor 2	95.4	97.8
Donor 3	90.3	97.1
Mean	93.7	97.7
s.e.m.	1.7	0.4

Mean memory Treg frequency with s.e.m. CD3CD4: clusters of differentiation 3 and 4; FoxP3: forkhead box protein P3; CD45RO: cluster of differentiation 45RO memory marker; s.e.m.: standard error of the mean; Tregs: regulatory T cells.

medium, and restimulated with soluble activator complex to allow the cells to recover from cryopreservation²⁸. Cell culture supernatants were assayed in triplicate for the production of IL-10 and TGF- β 1. As shown in Table 2, the mean IL-10 stimulation index was 164 (range 1–480) for flask-expanded Tregs and 1,287 (range 180–3,277) for the Quantum system-expanded Tregs across the three donor products, demonstrating a mean 8-fold increase in IL-10 secretion in the Quantum system perfusion-expanded Tregs over flask diffusion-based cell culture (Table 2). Across the three donor Treg populations, the unstimulated flask IL-10 secretion ranged from 7.1 to 935.6 pg/ml and stimulated flask IL-10 secretion ranged from 8.6 to 11,607.9 pg/ml. The unstimulated Quantum system IL-10 secretion ranged from 0.1 to 20.8 pg/ml and the stimulated Quantum IL-10 secretion ranged from 27.0 to 8,378.1 pg/ml. In contrast, the mean TGF- β 1 stimulation indices were similar between the two expansion methods and were essentially unchanged following stimulation. Across the three donor Treg populations, the unstimulated flask TGF- β 1 secretion ranged from 271.8 to 400.2 pg/ml and the stimulated flask TGF- β 1 secretion ranged from 289.4 to 679.2 pg/ml. In comparison, the unstimulated Quantum system TGF- β 1 secretion ranged from 288.5 to 363.4 pg/ml and the stimulated Quantum system TGF- β 1 secretion ranged from 271.9 to 304.7 pg/ml.

Treg In Vitro Suppression Assay

To prepare Tregs for the *in vitro* suppression assay, cryopreserved cells from Quantum system expansions were thawed,

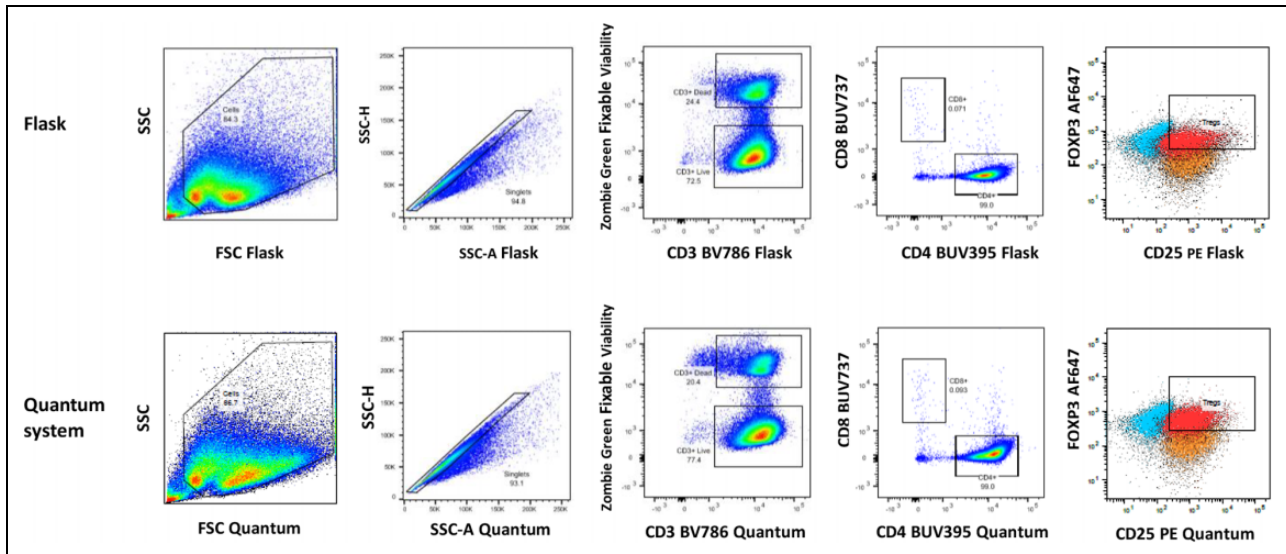


Figure 4. Example of flow cytometry gating strategy for phenotyping of Tregs in both flask and Quantum system Treg-harvested cells. Treg frequency is based on the number of CD4⁺CD25⁺FoxP3⁺ cells within the CD25⁺FoxP3⁺ double-positive gate that are above background FMO fluorescence for both FoxP3 and CD25. Flask gate labels, plots left to right: SSC vs FSC cells, singlets (SSC-H vs SSC-A), CD3⁺ dead and CD3⁺ live, CD8⁺ vs CD4⁺, CD25⁺FoxP3⁺ Tregs; Quantum system gate labels, plots left to right: SSC vs FSC cells, singlets (SSC-H vs SSC-A), CD3⁺ dead and CD3⁺ live, CD8⁺ vs CD4⁺, CD25⁺FoxP3⁺ Tregs. FoxP3 AF: 647; CD8 BUV: 737; CD3 BV: 786; CD4: BUV395; FMO: fluorescence minus one; FoxP3: forkhead box protein P3; FSC: forward scatter; PE: CD25; SSC: side scatter; SSC-A: side scatter - area; SSC-H: side scatter - height; Tregs: regulatory T cells.

Table 2. Post-expansion Treg Cytokine Secretion After Cryopreservation and Restimulation With Soluble Activator Complex.

Treg Cell Expansion	IL-10 Secretion (n = 3) Stimulation Index	TGF- β 1 Secretion (n = 3) Stimulation Index
Donor 1		
Flask	12	1
Quantum system	403	1
Donor 2		
Flask	1	2
Quantum system	180	1
Donor 3		
Flask	480	1
Quantum system	3,277	1
Mean flask	164	1
s.e.m.	158	0
Mean Quantum system	1,287	1
s.e.m.	997	0

The cytokine stimulation indices were normalized for each of the three donor cell products based on the stimulated values (pg/ml) divided by unstimulated values (pg/ml). IL-10: interleukin-10; s.e.m.: standard error of the mean; TGF- β 1: transforming growth factor- β 1; Tregs: regulatory T cells.

restimulated, and expanded *in vitro* for 5 d and for 13 d with IL-2 and antihuman CD28 mAb. The initial measurement of Treg viability immediately after thawing was between 69% and 74%, a mean of 73% for cells from all three donors (Fig. 5A). Viability dipped to a mean of 62% on day 1 and had reached 90% by day 5. Thereafter, viability stabilized between 75% and 90% out to 14 d (Fig. 5A).

To determine the functional characteristics of the cells, Tregs were placed in co-culture with con A–stimulated splenocytes isolated from GFP-expressing rats. GFP-rat splenocytes were mixed with Tregs at ratios of 1:1, 1:2, 1:4, 1:8, and 1:16. Suppressiveness of Tregs was measured from Tregs that had been cultured for 5 and 13 d prior to co-culture.

The quantity of GFP fluorescence over time was measured to determine the influence of co-cultured Tregs on the activated splenocytes. Tregs cultured for 5 d prior to coculture inhibited splenocyte expansion at all Treg:splenocyte ratios (Fig. 5B). Similar inhibition was observed when Tregs were cultured for 13 d prior to coculture (Fig. 5C). Interestingly, the degree of functional suppression of splenocyte expansion was greater with Tregs cultured for 13 d compared to those cultured for 5 d.

There was a correlation of Treg suppression to Treg harvest yield ($R^2 = 0.9979$) by linear regression across the three donor cell products, suggesting there was a relationship between their suppressive function on day 4 in splenocyte co-culture and cell proliferation of expanded Tregs in the Quantum system (Fig. 5D). The lack of correlation

between splenocyte suppression and IL-10 cytokine concentration in this experimental range suggests that there might be a cytokine threshold effect since all three Treg donor cell populations were shown to suppress splenocyte proliferation (Fig. 5E)²⁹.

To assess the immunophenotype of cells used in the rat splenocyte suppression assay, Tregs after 13 d of culture were labeled with antibodies specific for CD4, CD25, and FoxP3. Quantification performed as described in the Materials and Methods section showed that the cells were 96.55% CD4⁺, 95.32% CD25⁺, and 96.65% FoxP3⁺ (Fig. 5F).

Discussion

With respect to supporting cell transplantation and the control of autoimmune diseases, one of the challenges has been to generate a sufficient number of Tregs for a projected therapeutic dose since Tregs range from only 4% to 6% of bulk CD4⁺ T cells derived from either bone marrow or peripheral blood^{1,30,31}. The demand for this vital T cell subset will likely continue to be explored. As of spring 2020, ClinicalTrials.gov lists more than 900 clinical studies involving Tregs covering a broad spectrum of cell transplantation therapies and immunotherapies.

In the study reported here, we compared manual flask-based diffusion culture of Tregs with automated Quantum system perfusion-based cell culture in order to explore alternatives to conventional Treg expansion production for manufacturing cellular therapies under good manufacturing practices (GMP). We found that enriched Tregs from three healthy donors expanded 17.7-fold more on average and had improved viability when grown in the Quantum system compared to flask-based cultures. Moreover, average cell yields from Quantum systems, 7.0 billion Tregs, were within the projected clinical dose ranges reported in the literature for autologous Treg therapies, which range from 3 billion up to 5 billion^{5,6}. Variations in Treg yield across the three donors were observed but are to be expected and may be partially attributed to the degree of hypomethylation occurring in the promoter Treg-specific demethylated region of the master transcriptional factor FOXP3 gene, which is known to vary greatly among individuals (e.g., from 3.6% to 21.3%)^{32–34}. It is also well accepted that the pool of human FoxP3⁺ Tregs is heterogeneous and is dependent on different development conditions, anatomical locations, cytokine microenvironment, levels of transcription factors, mechanisms of suppression, surface biomarkers, and age of the individual^{35–38}. Harvested Tregs from both flasks and Quantum systems maintained a CD4⁺CD25⁺FoxP3⁺ Treg phenotype and memory CD4⁺CD25⁺FoxP3⁺CD45RO⁺ Treg phenotype considered important for maintenance of immune homeostasis^{39–42} with very high frequencies of these phenotypes at harvest. However, there was a trend toward higher mature Treg and activated Treg frequencies in Quantum system culture versus flask culture. We also chose a xenogeneic component-free, serum-free base medium that reportedly

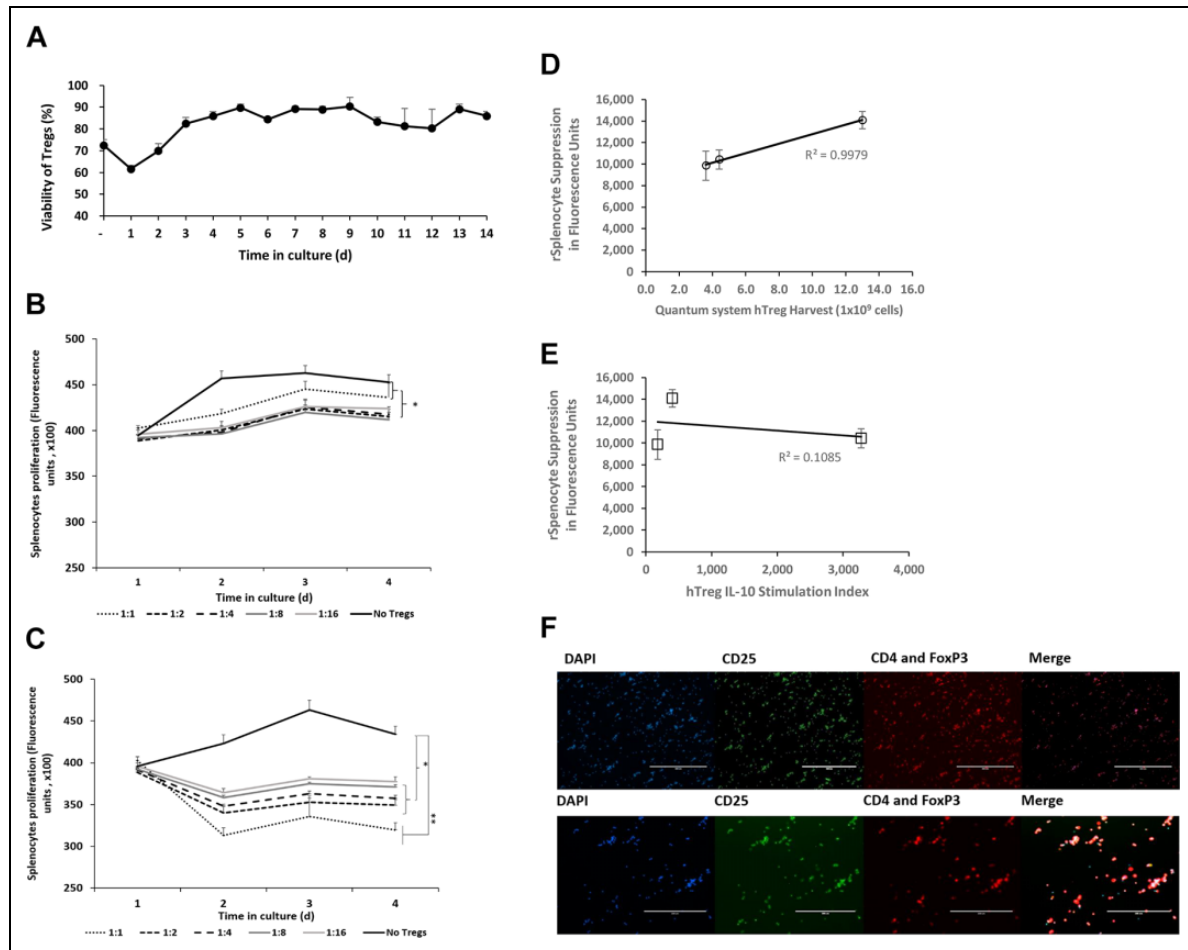


Figure 5. Tregs expanded in the Quantum system suppress proliferation of rat splenocytes. Mean viability for Tregs from the Quantum system, after cryopreservation and reculture ($n = 3$ donors) (A). *In vitro* immunosuppression of rat splenocyte proliferation elicited by Tregs from Quantum system expansions. Mean responses of GFP rat splenocytes cocultured with Tregs ($n = 3$ donors) after 5 d (B) or 13 d (C) postthaw ($*P < 0.05$, $**P < 0.005$ by Student's *t*-test). Correlation between maximum day 4 *in vitro* suppression of rat splenocyte proliferation and Quantum system Treg yield (D) and Treg IL-10 stimulation index (E). Fluorescent images of Tregs immunolabeled for CD4, CD25, and FoxP3 (F), scale: 200 (top) and 400 (bottom) μm . Error bars depict s.e.m. CD4: PE; CD25: Alexa 488; DAPI: 4', 6-diamidino-2-phenylindole; FoxP3: forkhead box protein P3; PE; GFP: green fluorescent protein; hTreg: human regulatory T cells; IL-10: interleukin-10; Tregs: regulatory T cells.

supports the expansion of memory T cells⁴³. In addition, the stimulation index for IL-10 secretion from harvested and restimulated Tregs was 8-fold higher in Quantum system-expanded Tregs than in flask-expanded Tregs. Taken together, these results indicate the advantage of the Quantum system over flask-based culture for expansion of functional Tregs.

Gas transfer in flasks is by passive diffusion, and the depth of the medium overlay in conventional cell culture systems limits the amount of oxygen that is available to cells. According to Fick's first law in cell culture, the diffusive flux of a gas is proportional to the concentration gradient which in turn is inversely proportional to the thickness of the liquid layer^{44,45}. The McMurtrey model of oxygen diffusion through overlying liquid medium is described by the

following equation, where J is the net flux of oxygen, l is the medium depth, P is the partial pressure of oxygen (in units of standard atmosphere), H is Henry's constant for the medium solution (in units of 1 atm/mol), C_0 is the concentration of oxygen, and D is the diffusivity coefficient for a molecule in a given medium⁴⁶:

$$J = \frac{-D}{l} \left(\frac{P}{H} - C_0 \right)$$

In this model, the net flux of oxygen is inversely related to medium depth. Hence, keeping the depth of medium as shallow as possible augments gas transfer during cell expansion. In our study, the depth of the medium in the Quantum system hollow-fiber bioreactor filled with 124 ml of medium is estimated to be 25-fold shallower than the depth in a T225

flask filled with the same volume. Therefore, the greatly enhanced expansion of Tregs in the Quantum system is likely due to increased availability of oxygen. Moreover, previous work has shown that Treg migration, proliferation, and suppressive function are supported by the presence of oxygen^{47,48}. Although we did not have the ability to measure oxygen consumed during our Treg cell expansion experiments, it has been shown that reduced oxygen levels associated with hypoxia may limit the generation of Tregs through the expression of Hif-1 α , a negative regulator of T cell responses⁴⁹. This may explain the higher percentage of FoxP3⁺ Tregs generated in the Quantum system versus flask-based culture as oxygen is likely to be more available in the Quantum system due to the increased surface area of the gas transfer module, which delivers oxygen to a hollow fiber bioreactor versus a single-chambered T-flask (225 cm²). Therefore, it is likely that both reduced media depth and increased gas transfer surface area, in the context of continuous media flow, play a role in rapidly establishing oxygen equilibrium during exponential cell growth in a perfusion bioreactor system⁵⁰.

In the study described here, we compared the diffusion-based culture in flasks, which utilizes bolus feeding, with perfusion-based culture, which utilizes continuous automated feeding. Tregs in a quiescent state utilize fatty acid oxidation (FAO) to supply the energy needed to maintain cell homeostasis⁵¹. Moreover, they are highly dependent on mitochondrial metabolism with the plasticity to oxidize lipid or glucose carbon sources^{52–54}. Upon stimulation, however, Tregs convert their metabolism to meet their energy and metabolite demands and have been shown to shift toward glycolysis^{55,56}. Automated feeding, coupled with gas perfusion, offers a continuous process for the support of stimulated-Treg metabolic conversion from FAO to glycolysis rather than the intermittent, diffusion-based feeding used in manual flask culture.

Other functionally closed expansion technologies that are semi- or fully automated are available for growth of cells for cellular therapies. For example, T cell immunotherapies such as chimeric antigen receptor T cells, tumor infiltrating lymphocytes, and T cell receptor-engineered T cells have been expanded in a variety of systems including the XuriTM W25 and WAVE Cell Expansion systems (GE Healthcare Life Sciences, Marlborough, MA, USA)^{57,58}, Gas Permeable Rapid Expansion (G-Rex) devices (Wilson Wolf Corporation, St. Paul, MN, USA)^{59,60}, the CliniMACS Prodigy (Miltenyi Biotec, GmbH, Germany)^{61–64}, and the Aastrom bioreactor (Aastrom BioSciences Inc., Ann Arbor, MI, USA)⁶⁵. To our knowledge, however, most publications describing expansion of Tregs for potential immunotherapies have to date utilized traditional culture methods such as flasks or cell culture bags⁶⁶. Two recent reports have demonstrated Treg expansions for clinical application in the G-Rex⁵ and in the Prodigy system⁶⁷ and data from these reports indicate that the Quantum system is comparable in terms of cell numbers achieved in similar timeframes and in

the high expression of Foxp3 and potent functionality of the Treg products.

A unique feature of the Quantum system is the dual loop system that allows for both efficient perfusion-based gas exchange and partitioning of different formulations and volumes of medium to the IC and EC fluid loops. In addition, the dual loop design has the potential to reduce use of cytokines and growth factors such as IL-2, since these can be preferentially added to the relatively small volume of IC medium only, with nutrient and gas supply provided from the EC side. Thus, in addition to the advantages over flask-based cell culture described here, the Quantum system has features that may be advantageous over other automated or semiautomated platforms for the generation of potent Tregs for use in immunotherapy.

Human Tregs are characterized by a symphony of responses depending on their microenvironment, including the secretion of inhibitory cytokines IL-10 and TGF- β 1 as well as the sequestering of IL-2²⁹. FoxP3⁺ Tregs that secrete IL-10 are especially relevant to regulating adaptive immune responses at the body's environmental interfaces^{68–71}. The stimulation index for IL-10 secretion from restimulated Tregs was 8-fold higher in Quantum system-expanded Tregs than in flask-expanded Tregs. In contrast, the stimulation index for TGF- β 1 in both cell culture processes remained unchanged, with secretion of TGF- β 1 being at very low levels. Together, the combination of an increased IL-10 secretion coupled with reduced TGF- β 1 secretion could represent the signature of proliferating Tregs that may be preferentially generated in the Quantum system⁷².

Our choice to use the anti-CD3/CD28/CD2 soluble antibody complex for stimulation of Tregs during expansion was based on a strategy to stimulate T cells in a uniform and complete manner as opposed to using antibody-conjugated beads, which tend to be sequestered in T cell aggregates. We elected to evaluate the use of anti-CD2 mAb as a costimulant in the complex based on reports of augmentation of T cell receptor/CD3 signaling by costimulation with anti-CD2 mAb⁷³. Moreover, a previously published study of the Treg signature also indicates that IL-2-responsive genes, such as the IL-2R α (CD25) receptor, are overexpressed in Tregs versus those expressed in T effector cells when activated in medium supplemented with IL-2⁷⁴. This profile further elucidates the need for a complete stimulation of Tregs during cell expansion through additional accessory molecules such as CD2.

Although some expansion protocols use rapamycin, an mTOR inhibitor, in the expansion of Tregs primarily to eliminate contaminating cell types, the T cell receptor and coreceptor CD28 signal through the mTOR complex 1 (mTORC1), which has a high level of activity in Tregs compared with effector T cells^{52,53,75}, and thus disruption of the mTORC1 pathway can result in the loss of Treg suppressive activity⁷⁶. In addition, mTORC1 signaling in Tregs promotes cholesterol and lipid metabolism and is particularly important for coordinating Treg growth and proliferation and

for the upregulation of suppressive molecules⁷⁵. We, therefore, elected to omit rapamycin from the medium formulation and to use enriched Tregs in our expansion study to prevent effector T cell outgrowth.

Functionality of Tregs expanded in the Quantum system was confirmed by the suppression of rat splenocyte proliferation. In our study, Treg suppression was also found to relate to the degree of cell expansion after cryopreservation, where Tregs cultured for 13 d were more suppressive than those cultured for 5 d. While a likely cause is that the cryopreserved Tregs required some time to reestablish proliferation and functional characteristics after thawing, we do not yet know the mechanisms responsible which could explain the mechanism of splenocyte suppression. However, the degree of functional inhibition by Tregs shown here is consistent with the previous characterization of Treg functionality across multiple species, including xenogeneically^{24,40,77,78}.

Although the current mechanism of suppression in the xenogeneic context is not yet elucidated, it may be manifested by Treg secretion of IL-10. The rat IL-10 receptor protein has a reported 61% homology to the human IL-10 receptor proteins⁷⁹. Other studies have demonstrated the functionality of human IL-10 in rat models. Johnston et al. have shown that human IL-10, delivered by an adeno-associated viral vector, is protective in a rat model of Parkinson's disease, and Fakin et al. have demonstrated the amelioration of lung allograft rejection by sequential overexpression of human IL-10 and hepatocyte growth factor in a rat model^{80,81}. As part of their suppressive repertoire, Tregs are also known to sequester or to provide a "sink" for exogenous IL-2^{82–85}. Overall, suppression assays with expanded human Tregs in animal models may have additional utility in the translation of preclinical results to clinical transplantation studies⁸³.

Considering the Treg expansion yield, viability, memory phenotype preservation, and functional performance, the perfusion-based Quantum system shows promise in the scale-up of Tregs for therapeutic indications as demonstrated here and appears to represent an improvement over manual flask-based culture. In addition, we have defined an automated method for Treg expansion using a soluble activator complex in serum-free medium, additional features that are likely to be desirable for production of Tregs under GMP for clinical indications⁶⁶.

Acknowledgments

We thank Dr Kimberley Jordan of the Human Immune Monitoring Shared Resource, Department of Immunology and Microbiology, University of Colorado School of Medicine, Aurora, CO, USA, for the flow cytometry phenotyping and functional assays of the Tregs expanded in the Quantum System and flask studies.

Ethical Approval

Animals were acquired, cared for, and used in accordance with the NIH Guide for the Care and Use of Laboratory Animals, and a

protocol approved by the University of Wyoming Institutional Animal Care and Use Committee, Laramie, WY, USA, was followed.

Statement of Animal Rights

All of the experimental procedures involving animals were conducted in accordance with the Institutional Animal Care Guidelines of the University of Wyoming, Laramie, WY, USA, and were approved by the Institutional Animal Care and Use Committee of the University of Wyoming.

Statement of Informed Consent

There are no human subjects in this article and informed consent is not applicable. Donor cells were collected by the vendor, STEMCELL Technologies, in accordance with local, state, and federal U.S. requirements and were obtained from normal or non-infectious diseased donors voluntarily participating in a donor program with consent that is approved by an institutional review board, FDA, or an equivalent regulatory agency.


Declaration of Conflicting Interests

The author(s) declared the following potential conflicts of interest with respect to the research, authorship, and/or publication of this article: M. Jones, B. Nankervis, and C. Coeshott are employees of Terumo BCT, Inc. (Lakewood, CO, USA). J. Bushman, K. Roballo, and H. Pham are in the School of Pharmacy at the University of Wyoming (Laramie, WY, USA). None of the authors has any competing financial interests to declare.

Funding

The author(s) received no financial support for the research, authorship, and/or publication of this article.

ORCID iD

Mark Jones  <https://orcid.org/0000-0001-7572-5274>

References

- Blache C, Chauvin JM, Marie-Cardine A, Contentin N, Pommier P, Dedreux I, Francois S, Jacquot S, Bastit D, Boyer O. Reduced frequency of regulatory T cells in peripheral blood stem cell compared to bone marrow transplantations. *Biol Blood Marrow Transplant*. 2010;16(3):430–434.
- Bluestone JA, Tang Q. Treg cells—the next frontier of cell therapy. *Science*. 2018;362(6411):154–155.
- Esensten JH, Muller YD, Bluestone JA, Tang Q. Regulatory T-cell therapy for autoimmune and autoinflammatory diseases: the next frontier. *J Allergy Clin Immunol*. 2018;142(6):1710–1718.
- Ferreira LMR, Muller YD, Bluestone JA, Tang Q. Next-generation regulatory T cell therapy. *Nat Rev Drug Discov*. 2019;18(10):749–769.
- Mathew JM, Voss JH, LeFever A, Konieczna I, Stratton C, He J, Huang X, Gallon L, Skaro A, Ansari MJ, Leventhal JR. A phase I clinical trial with ex vivo expanded recipient regulatory T cells in living donor kidney transplants. *Sci Rep*. 2018;8(1):7428.
- Bluestone JA, Buckner JH, Fitch M, Gitelman SE, Gupta S, Hellerstein MK, Herold KC, Lares A, Lee MR, Li K, Tang Q.

- Type 1 diabetes immunotherapy using polyclonal regulatory T cells. *Sci Transl Med.* 2015;7(315):315ra189.
7. Coeshott C, Vang B, Jones M, Nankervis B. Large-scale expansion and characterization of CD3(+) T-cells in the Quantum((R)) Cell Expansion System. *J Transl Med.* 2019;17(1):258.
 8. Nankervis B, Jones M, Vang B, Brent Rice R, Jr., Coeshott C, Beltzer J. Optimizing T cell expansion in a Hollow-Fiber bioreactor. *Curr Stem Cell Rep.* 2018;4(1):46–51.
 9. Liu W, Putnam AL, Xu-Yu Z, Szot GL, Lee MR, Zhu S, Gottlieb PA, Kapranov P, Gingeras TR, Fazekas de St Groth B, Bluestone JA. CD127 expression inversely correlates with FoxP3 and suppressive function of human CD4+ T reg cells. *J Exp Med.* 2006;203(7):1701–1711.
 10. Peters JH, Preijers FW, Woestenenk R, Hilbrands LB, Koenen HJ, Joosten I. Clinical grade Treg: GMP isolation, improvement of purity by CD127 Depletion, Treg expansion, and Treg cryopreservation. *PLoS One.* 2008;3(9):e3161.
 11. Trzonkowski P, Bieniaszewska M, Juscinska J, Dobyszyk A, Krzystyniak A, Marek N, Mysliwska J, Hellmann A. First-in-man clinical results of the treatment of patients with graft versus host disease with human ex vivo expanded CD4+CD25+CD127- T regulatory cells. *Clin Immunol.* 2009;133(1):22–26.
 12. van der Net JB, Bushell A, Wood KJ, Harden PN. Regulatory T cells: first steps of clinical application in solid organ transplantation. *Transpl Int.* 2016;29(1):3–11.
 13. van der Windt GJ, Pearce EL. Metabolic switching and fuel choice during T-cell differentiation and memory development. *Immunol Rev.* 2012;249(1):27–42.
 14. Gingras AC, Raught B, Sonenberg N. Regulation of translation initiation by FRAP/mTOR. *Genes Dev.* 2001;15(7):807–826.
 15. Kim DH, Sarbassov DD, Ali SM, King JE, Latek RR, Erdjument-Bromage H, Tempst P, Sabatini DM. mTOR interacts with raptor to form a nutrient-sensitive complex that signals to the cell growth machinery. *Cell.* 2002;110(2):163–175.
 16. Chapman NM, Chi H. mTOR signaling, Tregs and immune modulation. *Immunotherapy.* 2014;6(12):1295–1311.
 17. Fraser H, Safinia N, Grageda N, Thirkell S, Lowe K, Fry LJ, Scotta C, Hope A, Fisher C, Hilton R, Lombardi G. A Rapamycin-based GMP-compatible process for the isolation and expansion of regulatory T cells for clinical trials. *Mol Ther Methods Clin Dev.* 2018;8:198–209.
 18. He X, Landman S, Bauland SC, van den Dolder J, Koenen HJ, Joosten I. A TNFR2-agonist facilitates high purity expansion of human low purity Treg cells. *PLoS One.* 2016;11(5):e0156311.
 19. Fowler DH. Rapamycin-resistant effector T-cell therapy. *Immunol Rev.* 2014;257(1):210–225.
 20. Gedaly R, De Stefano F, Turcios L, Hill M, Hidalgo G, Mitov MI, Alstott MC, Butterfield DA, Mitchell HC, Hart J, Marti F. mTOR inhibitor Everolimus in regulatory T cell expansion for clinical application in transplantation. *Transplantation.* 2019;103(4):705–715.
 21. Fingar DC, Salama S, Tsou C, Harlow E, Blenis J. Mammalian cell size is controlled by mTOR and its downstream targets S6K1 and 4EBP1/eIF4E. *Genes Dev.* 2002;16(12):1472–1487.
 22. Fuchs A, Gliwinski M, Grageda N, Spiering R, Abbas AK, Appel S, Bacchetta R, Battaglia M, Berglund D, Blazar B, Hester J, et al. Minimum information about T regulatory cells: a step toward reproducibility and standardization. *Front Immunol.* 2017;8:1844.
 23. Sherley JL, Stadler PB, Stadler JS. A quantitative method for the analysis of mammalian cell proliferation in culture in terms of dividing and non-dividing cells. *Cell Prolif.* 1995;28(3):137–144.
 24. Roballo KC, Dhungana S, Jiang Z, Oakey J, Bushman J. Localized delivery of immunosuppressive regulatory T cells to peripheral nerve allografts promotes regeneration of branched segmental defects. *Biomaterials.* 2019;209:1–9.
 25. Lois C, Hong EJ, Pease S, Brown EJ, Baltimore D. Germline transmission and tissue-specific expression of transgenes delivered by lentiviral vectors. *Science.* 2002;295(5556):868–872.
 26. Men H, Bauer BA, Bryda EC. Germline transmission of a novel rat embryonic stem cell line derived from transgenic rats. *Stem Cells Dev.* 2012;21(14):2606–2612.
 27. Onishi Y, Fehervari Z, Yamaguchi T, Sakaguchi S. Foxp3+ natural regulatory T cells preferentially form aggregates on dendritic cells *in vitro* and actively inhibit their maturation. *Proc Natl Acad Sci U S A.* 2008;105(29):10113–10118.
 28. Golab K, Leveson-Gower D, Wang XJ, Grzanka J, Marek-Trzonkowska N, Krzystyniak A, Millis JM, Trzonkowski P, Witkowski P. Challenges in cryopreservation of regulatory T cells (Tregs) for clinical therapeutic applications. *Int Immunopharmacol.* 2013;16(3):371–375.
 29. Chaudhry A, Samstein RM, Treuting P, Liang Y, Pils MC, Heinrich JM, Jack RS, Wunderlich FT, Bruning JC, Muller W, Rudensky AY. Interleukin-10 signaling in regulatory T cells is required for suppression of Th17 cell-mediated inflammation. *Immunity.* 2011;34(4):566–578.
 30. Su LF, Del Alcazar D, Stelekati E, Wherry EJ, Davis MM. Antigen exposure shapes the ratio between antigen-specific Tregs and conventional T cells in human peripheral blood. *Proc Natl Acad Sci U S A.* 2016;113(41):E6192–E6198.
 31. Liotta F, Gacci M, Frosali F, Querci V, Vittori G, Lapini A, Santarlasci V, Serni S, Cosmi L, Maggi L, Annunziato F. Frequency of regulatory T cells in peripheral blood and in tumour-infiltrating lymphocytes correlates with poor prognosis in renal cell carcinoma. *BJU Int.* 2011;107(9):1500–1506.
 32. Bending D, Pesenacker AM, Ursu S, Wu Q, Lom H, Thirugnanabalan B, Wedderburn LR. Hypomethylation at the regulatory T cell-specific demethylated region in CD25hi T cells is decoupled from FOXP3 expression at the inflamed site in childhood arthritis. *J Immunol.* 2014;193(6):2699–2708.
 33. Shimazu Y, Shimazu Y, Hishizawa M, Hamaguchi M, Nagai Y, Sugino N, Fujii S, Kawahara M, Kadowaki N, Nishikawa H, Takaori-Kondo A. Hypomethylation of the Treg-specific Demethylated region in FOXP3 Is a hallmark of the regulatory

- T-cell subtype in adult T-cell Leukemia. *Cancer Immunol Res.* 2016;4(2):136–145.
34. Afzali B, Edozie FC, Fazekasova H, Scotta C, Mitchell PJ, Canavan JB, Kordasti SY, Chana PS, Ellis R, Lord GM, Lombardi G. Comparison of regulatory T cells in hemodialysis patients and healthy controls: implications for cell therapy in transplantation. *Clin J Am Soc Nephrol.* 2013;8(8):1396–1405.
 35. Mohr A, Malhotra R, Mayer G, Gorochov G, Miyara M. Human FOXP3(+) T regulatory cell heterogeneity. *Clin Transl Immunology.* 2018;7(1):e1005.
 36. Kinoshita M, Kobayashi S, Gotoh K, Kubo M, Hayashi K, Iwagami Y, Yamada D, Akita H, Noda T, Asaoka T, Doki Y. Heterogeneity of Treg/Th17 according to cancer progression and modification in Biliary tract cancers via self-producing cytokines. *Dig Dis Sci.* 2019 (Dec 18); DOI: 10.1007/s10620-019-06011-9.
 37. Min B. Heterogeneity and stability in Foxp3+ regulatory T cells. *J Interferon Cytokine Res.* 2017;37(9):386–397.
 38. Shevryev D, Tereshchenko V. Treg heterogeneity, function, and homeostasis. *Front Immunol.* 2020;10:3100.
 39. Miyara M, Yoshioka Y, Kitoh A, Shima T, Wing K, Niwa A, Parizot C, Taflin C, Heike T, Valeyre D, Sakaguchi S. Functional delineation and differentiation dynamics of human CD4+ T cells expressing the FoxP3 transcription factor. *Immunity.* 2009;30(6):899–911.
 40. Ballke C, Gran E, Baekkevold ES, Jahnsen FL. Characterization of regulatory T-Cell markers in CD4+ T cells of the upper airway Mucosa. *PLoS One.* 2016;11(2):e0148826.
 41. Rosenblum MD, Way SS, Abbas AK. Regulatory T cell memory. *Nat Rev Immunol.* 2016;16(2):90–101.
 42. Safinia N, Grageda N, Scotta C, Thirkell S, Fry LJ, Vaikunthanathan T, Lechler RI, Lombardi G. Cell therapy in organ transplantation: our experience on the clinical translation of regulatory T cells. *Front Immunol.* 2018;9:354.
 43. Kumar P, Marinelarena A, Raghunathan D, Ragothaman VK, Saini S, Bhattacharya P, Fan J, Epstein AL, Maker AV, Prabhakar BS. Critical role of OX40 signaling in the TCR-independent phase of human and murine Thymic Treg generation. *Cell Mol Immunol.* 2019;16(2):138–153.
 44. Al-Ani A, Toms D, Kondro D, Thundathil J, Yu Y, Ungrin M. Oxygenation in cell culture: critical parameters for reproducibility are routinely not reported. *PLoS One.* 2018;13(10):e0204269.
 45. Place TL, Domann FE, Case AJ. Limitations of oxygen delivery to cells in culture: an underappreciated problem in basic and translational research. *Free Radic Biol Med.* 2017;113:311–322.
 46. McMurtrey RJ. Analytic models of oxygen and nutrient diffusion, metabolism dynamics, and architecture optimization in three-dimensional tissue constructs with applications and insights in cerebral Organoids. *Tissue Eng Part C Methods.* 2016;22(3):221–249.
 47. Kishore M, Cheung KCP, Fu H, Bonacina F, Wang G, Coe D, Ward EJ, Colamatteo A, Jangani M, Baragetti A, Marelli-Berg FM. Regulatory T cell migration is dependent on Glucokinase-mediated glycolysis. *Immunity.* 2017;47(5):875–889.
 48. Miska J, Lee-Chang C, Rashidi A, Muroski ME, Chang AL, Lopez-Rosas A, Zhang P, Panek WK, Cordero A, Han Y, Lesniak MS. HIF-1alpha is a metabolic switch between Glycolytic-driven migration and Oxidative phosphorylation-driven immunosuppression of tregs in Glioblastoma. *Cell Rep.* 2019;27(1):226–237.
 49. McNamee EN, Korn Johnson D, Homann D, Clambey ET. Hypoxia and hypoxia-inducible factors as regulators of T cell development, differentiation, and function. *Immunol Res.* 2013;55(1-3):58–70.
 50. Jones M, Nankervis B, Frank N, Vang B, DiLorenzo T. CD146 expression, as a surrogate biomarker for human mesenchymal stromal cell multilineage differentiation, is preserved during cell expansion in an automated hollow-fiber membrane bioreactor. *Pharmaceutical Bioprocessing.* 2018;6(3):93–105.
 51. Pacella I, Procaccini C, Focaccetti C, Miacci S, Timperi E, Faicchia D, Severa M, Rizzo F, Coccia EM, Bonacina F, Picone S. Fatty acid metabolism complements glycolysis in the selective regulatory T cell expansion during tumor growth. *Proc Natl Acad Sci USA.* 2018;115(28):E6546–E6555.
 52. Galgani M, De Rosa V, La Cava A, Matarese G. Role of metabolism in the immunobiology of regulatory T cells. *J Immunol.* 2016;197(7):2567–2575.
 53. Almeida L, Lochner M, Berod L, Sparwasser T. Metabolic pathways in T cell activation and lineage differentiation. *Semin Immunol.* 2016;28(5):514–524.
 54. He N, Fan W, Henriquez B, Yu RT, Atkins AR, Liddle C, Zheng Y, Downes M, Evans RM. Metabolic control of regulatory T cell (Treg) survival and function by Lkb1. *Proc Natl Acad Sci USA.* 2017;114(47):12542–12547.
 55. Newton R, Priyadarshini B, Turka LA. Immunometabolism of regulatory T cells. *Nat Immunol.* 2016;17(6):618–665.
 56. Wang R, Dillon CP, Shi LZ, Milasta S, Carter R, Finkelstein D, McCormick LL, Fitzgerald P, Chi H, Munger J, Green DR. The transcription factor Myc controls metabolic reprogramming upon T lymphocyte activation. *Immunity.* 2011;35(6):871–882.
 57. Somerville RP, Devillier L, Parkhurst MR, Rosenberg SA, Dudley ME. Clinical scale rapid expansion of lymphocytes for adoptive cell transfer therapy in the WAVE(R) bioreactor. *J Transl Med.* 2012;10:69.
 58. Hollyman D, Stefanski J, Przybylowski M, Bartido S, Borquez-Ojeda O, Taylor C, Yeh R, Capacio V, Olszewska M, Hosey J, Riviere I. Manufacturing validation of biologically functional T cells targeted to CD19 antigen for autologous adoptive cell therapy. *J Immunother.* 2009;32(2):169–180.
 59. Vera JF, Brenner LJ, Gerdemann U, Ngo MC, Sili U, Liu H, Wilson J, Dotti G, Heslop HE, Leen AM, Rooney CM. Accelerated production of antigen-specific T cells for preclinical and clinical applications using gas-permeable rapid expansion cultureware (G-Rex). *J Immunother.* 2010;33(3):305–315.
 60. Jin J, Gkitsas N, Fellowes VS, Ren J, Feldman SA, Hinrichs CS, Stroncek DF, Highfill SL. Enhanced clinical-scale manufacturing of TCR transduced T-cells using closed culture system modules. 2018;16(1):13.

61. Mock U, Nickolay L, Philip B, Cheung GW, Zhan H, Johnston IC, Kaiser AD, Peggs K, Pule M, Thrasher AJ, Qasim W. Automated manufacturing of chimeric antigen receptor T cells for adoptive immunotherapy using CliniMACS prodigy. *Cytotherapy*. 2016;18(8):1002–1011.
62. Priesner C, Aleksandrova K, Esser R, Mockel-Tenbrinck N, Leise J, Drechsel K, Marburger M, Quaiser A, Goudeva L, Arseniev L, Koehl U. Automated enrichment, transduction, and expansion of clinical-scale CD62L(+) T cells for manufacturing of gene therapy medicinal products. *Hum Gene Ther*. 2016;27(10):860–869.
63. Zhang W, Jordan KR, Schulte B, Purev E. Characterization of clinical grade CD19 chimeric antigen receptor T cells produced using automated CliniMACS Prodigy system. *Drug Des Devel Ther*. 2018;12:3343–3356.
64. Lock D, Mockel-Tenbrinck N, Drechsel K, Barth C, Mauer D, Schaser T, Kolbe C, Al Rawashdeh W, Brauner J, Hardt O, Kaiser A. Automated manufacturing of potent CD20-directed chimeric antigen receptor T cells for clinical use. *Hum Gene Ther*. 2017;28(10):914–925.
65. Klapper JA, Thomasian AA, Smith DM, Gorgas GC, Wunderlich JR, Smith FO, Hampson BS, Rosenberg SA, Dudley ME. Single-pass, closed-system rapid expansion of lymphocyte cultures for adoptive cell therapy. *J Immunol Methods*. 2009;345(1-2):90–99.
66. MacDonald K PJ, Levings M. Methods to manufacture regulatory T cells for cell therapy. *Clinical and Experimental Immunology*. 2019;197(1):52–63.
67. Marin Morales JM, Munch N, Peter K, Freund D, Oelschlagel U, Holig K, Bohm T, Flach AC, Kessler J, Bonifacio E, Fuchs A. Automated clinical grade expansion of regulatory T cells in a fully closed system. *Front Immunol*. 2019;10:38.
68. Ng TH, Britton GJ, Hill EV, Verhagen J, Burton BR, Wraith DC. Regulation of adaptive immunity; the role of interleukin-10. *Front Immunol*. 2013;4:129.
69. Coombes JL, Robinson NJ, Maloy KJ, Uhlig HH, Powrie F. Regulatory T cells and intestinal homeostasis. *Immunol Rev*. 2005;204:184–194.
70. Maynard CL, Harrington LE, Janowski KM, Oliver JR, Zindl CL, Rudensky AY, Weaver CT. Regulatory T cells expressing interleukin 10 develop from Foxp3+ and Foxp3- precursor cells in the absence of interleukin 10. *Nat Immunol*. 2007;8(9):931–941.
71. Rubtsov YP, Rasmussen JP, Chi EY, Fontenot J, Castelli L, Ye X, Treuting P, Siewe L, Roers A, Henderson WR, Jr., Rudensky AY. Regulatory T cell-derived interleukin-10 limits inflammation at environmental interfaces. *Immunity*. 2008;28(4):546–558.
72. Gutcher I, Donkor MK, Ma Q, Rudensky AY, Flavell RA, Li MO. Autocrine transforming growth factor-beta1 promotes in vivo Th17 cell differentiation. *Immunity*. 2011;34(3):396–408.
73. Berney SM, Schaan T, Wolf RE, van der Heyde H, Atkinson TP. CD2 (OKT11) augments CD3-mediated intracellular signaling events in human T lymphocytes. *J Investig Med*. 2000;48(2):102–109.
74. Hill JA, Feuerer M, Tash K, Haxhinasto S, Perez J, Melamed R, Mathis D, Benoist C. Foxp3 transcription-factor-dependent and -independent regulation of the regulatory T cell transcriptional signature. *Immunity*. 2007;27(5):786–800.
75. Wawman RE, Bartlett H, Oo YH. Regulatory T cell metabolism in the hepatic microenvironment. *Front Immunol*. 2017;8:1889.
76. Zeng B, Kwak-Kim J, Liu Y, Liao AH. Treg cells are negatively correlated with increased memory B cells in pre-eclampsia while maintaining suppressive function on autologous B-cell proliferation. *Am J Reprod Immunol*. 2013;70(6):454–463.
77. Sakaguchi S, Sakaguchi N, Asano M, Itoh M, Toda M. Immunologic self-tolerance maintained by activated T cells expressing IL-2 receptor alpha-chains (CD25). Breakdown of a single mechanism of self-tolerance causes various autoimmune diseases. *J Immunol*. 1995;155(3):1151–1164.
78. Sakaguchi S, Sakaguchi N, Shimizu J, Yamazaki S, Sakihama T, Itoh M, Kuniyasu Y, Nomura T, Toda M, Takahashi T. Immunologic tolerance maintained by CD25+ CD4+ regulatory T cells: their common role in controlling autoimmunity, tumor immunity, and transplantation tolerance. *Immunol Rev*. 2001;182:18–32.
79. Ward H, Vignes S, Poole S, Bristow AF. The rat interleukin 10 receptor: cloning and sequencing of cDNA coding for the alpha-chain protein sequence, and demonstration by western blotting of expression in the rat brain. *Cytokine*. 2001;15(5):237–240.
80. Johnston LC, Su X, Maguire-Zeiss K, Horovitz K, Ankoudinova I, Guschin D, Hadaczek P, Federoff HJ, Bankiewicz K, Forsayeth J. Human interleukin-10 gene transfer is protective in a rat model of Parkinson's disease. *Mol Ther*. 2008;16(8):1392–1399.
81. Fakin R, Hamacher J, Gugger M, Gazdhar A, Moser H, Schmid RA. Prolonged amelioration of acute lung allograft rejection by sequential overexpression of human interleukin-10 and hepatocyte growth factor in rats. *Exp Lung Res*. 2011;37(9):555–562.
82. Nedoszytko B, Lange M, Sokolowska-Wojdylo M, Renke J, Trzonkowski P, Sobjanek M, Szczerkowska-Dobosz A, Niedozytko M, Gorska A, Romantowski J, Nowicki R. The role of regulatory T cells and genes involved in their differentiation in pathogenesis of selected inflammatory and neoplastic skin diseases. Part I: Treg properties and functions. *Postepy Dermatol Alergol*. 2017;34(4):285–294.
83. Zemmour D, Zilionis R, Kiner E, Klein AM, Mathis D, Benoist C. Single-cell gene expression reveals a landscape of regulatory T cell phenotypes shaped by the TCR. *Nat Immunol*. 2018;19(3):291–301.
84. Rudensky AY. Regulatory T cells and Foxp3. *Immunol Rev*. 2011;241(1):260–268.
85. Nish SA, Schenten D, Wunderlich FT, Pope SD, Gao Y, Hoshi N, Yu S, Yan X, Lee HK, Pasman L, Medzhitov R. T cell-intrinsic role of IL-6 signaling in primary and memory responses. *Elife*. 2014;3:1–21.